FEBS 24247 FEBS Letters 484 (2000) 139–143

Two-electron reduction and one-electron oxidation of organic hydroperoxides by human myeloperoxidase

Paul Georg Furtmüller, Ursula Burner, Walter Jantschko, Günther Regelsberger, Christian Obinger*

Institute of Chemistry, University of Agricultural Sciences, Muthgasse 18, A-1190 Vienna, Austria

Received 2 October 2000; accepted 3 October 2000

First published online 19 October 2000

Edited by Barry Halliwell

Abstract The reaction of native myeloperoxidase (MPO) and its redox intermediate compound I with hydrogen peroxide, ethyl hydroperoxide, peroxyacetic acid, *t*-butyl hydroperoxide, 3-chloroperoxybenzoic acid and cumene hydroperoxide was studied by multi-mixing stopped-flow techniques. Hydroperoxides are decomposed by MPO by two mechanisms. Firstly, the hydroperoxide undergoes a two-electron reduction to its corresponding alcohol and heme iron is oxidized to compound I. At pH 7 and 15°C, the rate constant of the reaction between 3-chloroperoxybenzoic acid and ferric MPO was similar to that with hydrogen peroxide (1.8×10^7 M^{-1} s^{-1} and 1.4×10^7 M^{-1} s^{-1}, respectively). With the exception of *t*-butyl hydroperoxide, the rates of compound I formation varied between 5.2×10^5 M^{-1} s^{-1} and 2.7×10^6 M^{-1} s^{-1}. Secondly, compound I can abstract hydrogen from these peroxides, producing peroxyl radicals and compound II. Compound I reduction is shown to be more than two orders of magnitude slower than compound I formation. Again, with 3-chloroperoxybenzoic acid this reaction is most effective (6.6×10^4 M^{-1} s^{-1} at pH 7 and 15°C). Both reactions are controlled by the same ionizable group (average pK_a of about 4.0) which has to be in its conjugated base form for reaction. **© 2000 Federation of European Biochemical Societies. Published by Elsevier Science B.V. All rights reserved.**

Key words: Myeloperoxidase; Compound I; Compound II; Superoxide; Peroxyl radical; Stopped-flow spectroscopy

1. Introduction

Myeloperoxidase (MPO) is a major neutrophil protein and is also present in monocytes. In neutrophils, it is stored in azurophilic granules and released during phagocytosis [1]. It is a heme enzyme that uses hydrogen peroxide generated by the neutrophil oxidative burst to produce hypochlorous acid and other reactive intermediates [1]. Since the MPO system has been demonstrated to be strongly bactericidal [2], the enzyme is considered as an important component of the neutrophil's antimicrobial armory. It has also been implicated in promoting tissue damage in numerous inflammatory diseases.

MPO is a member of the homologous mammalian peroxidase family (superfamily II) also including eosinophil peroxidase and thyroid peroxidase [3]. These peroxidases greatly differ from those isolated from plant, fungal and bacterial sources (superfamily I) in both primary, secondary, and tertiary structure as well as in having a covalent linkage of the heme group to the protein matrix [4]. MPO itself differs significantly from the other mammalian enzymes not only by its spectral characteristics but also because it is the only member of this group that is able to catalyze the oxidation of chloride into hypochlorite at a significant rate [5].

Of the oxidized intermediates of MPO, compound I is the only species that takes part in both the peroxidatic cycle and the chlorination activity. Compound I of MPO has some unusual features. An excess of hydrogen peroxide is necessary for its formation, it is very unstable and decays to its one-electron reduction product, compound II. There are three papers that elucidated the reactivity of MPO towards H_2O_2. Two studies were performed on the human enzyme [6,7], and a third on the beef spleen enzyme [8]. Similar results were obtained and the main features can be summarized in the following mechanism:

$$\text{MPO} + \text{H}_2\text{O}_2 \rightarrow \text{MPO-I} + \text{H}_2\text{O} \quad (1)$$

$$\text{MPO-I} + \text{H}_2\text{O}_2 \rightarrow \text{MPO-II} + \text{HO}_2^{\bullet} \quad (2)$$

with MPO-I and MPO-II being compounds I and II, respectively, and $HO_2^{\bullet}$ being the protonated form of superoxide. The reversibility of Reaction 1 was suggested to cause the large excess of hydrogen peroxide which is required to complete the formation of compound I [8]. Thus, compound I of MPO should be able to oxidize water to hydrogen peroxide. Evidence for Reaction 2 has been demonstrated with cytochrome *c* [7] and tetranitromethane [8] as superoxide scavenger.

Hydroperoxides have a profound influence on many cellular structures and functions. In many cases it is unknown whether these effects can be attributed to the hydroperoxide itself or to catalytic decomposition products, such as alkoxyl and peroxyl radicals which are thought to be formed intracellularly in reactions between hydroperoxides and heme proteins. Based on previous electron spin resonance studies that organic hydroperoxides are decomposed to free radicals by both neutrophils and purified MPO [9], we started a transient-state kinetic investigation to elucidate how organic peroxides are metabolized by MPO. Here we present apparent bimolecular rate constants and their pH dependence of compound I formation by hydrogen peroxide, ethyl hydroperoxide, peroxyacetic acid

*Corresponding author. Fax: (43)-1-36006 6059.
E-mail: cobinger@edv2.boku.ac.at

Abbreviations: MPO, myeloperoxidase; MPO-I, compound I; MPO-II, compound II; 3-CPBA, 3-chloroperoxybenzoic acid; PAA, peroxyacetic acid

0014-5793/00/$20.00 © 2000 Federation of European Biochemical Societies. Published by Elsevier Science B.V. All rights reserved.
PII: S0014-5793(00)02143-8

(PAA), *t*-butyl hydroperoxide, *m*-chloroperoxybenzoic acid and cumene hydroperoxide. We demonstrate that all investigated organic hydroperoxides can also function as one-electron donors of compound I. The corresponding apparent rate constants as well as their pH dependence are presented.

2. Materials and methods

2.1. Materials

MPO purification from human blood to a purity index (A_{430}/A_{280}) of at least 0.85 and determination of its concentration and that of hydrogen peroxide was performed as reported previously [5]. Organic peroxides and other chemicals were purchased from Sigma Chemical Co. at the highest grade available. Peroxide stock solutions were prepared freshly half-daily.

2.2. Methods

2.2.1. Transient-state kinetics. The sequential stopped-flow apparatus (model SX-18MV) and the associated computer system were from Applied Photophysics (UK). For a total of 100 μl/shot into a flow cell with 1 cm light path, the fastest time for mixing two solutions and recording the first data point was about 1.5 ms. Conventional stopped-flow analysis was used to monitor the reaction of the native ferric enzyme with organic hydroperoxides at 433 nm (i.e. the isosbestic point between compound I and compound II). Elucidation of pH dependence of compound I formation was performed by mixing MPO (1 μM heme) in 5 mM phosphate buffer (pH 7.0) with peroxides in 200 mM carbonate buffer (pH 8–9), 200 mM phosphate buffer (pH 7–8) or 200 mM citrate–phosphate buffer (pH 3–7). The final pH after mixing was controlled at the outlet.

Because of the inherent instability of MPO compound I [5], sequential stopped-flow (multi-mixing) analysis was used for determination of rates of the reaction of compound I with hydroperoxides at 456 nm, the Soret maximum of compound II. Parameters of formation and stability of compound I were as described previously by Furtmüller et al. [5]. The pH jump technique was used to investigate the pH dependence of compound II formation.

In a typical pH jump experiment, MPO (2 μM heme) in 5 mM buffer was premixed with 20 μM H_2O_2 in distilled water. After a delay time of 20 ms, compound I was allowed to react with varying concentrations of peroxide in 200 mM carbonate buffer (pH 8–9), 200 mM phosphate buffer (pH 7–8) or 200 mM citrate–phosphate buffer (pH 3–7).

At least three determinations (2000 data points) of pseudo-first-order rate constants (k_{obs}) were performed for each substrate concentration and the mean value was used in the calculation of the second-order rate constants, which were calculated from the slope of the line defined by a plot of k_{obs} versus substrate concentration. To allow calculation of pseudo-first-order rates, the concentrations of substrates were at least 10 times that of the enzyme. All reactions were performed at 15°C and followed both at single wavelengths as well as with a diode-array detector (PD1, Applied Photophysics). Typically, the heme concentration used in these experiments was 2 μM.

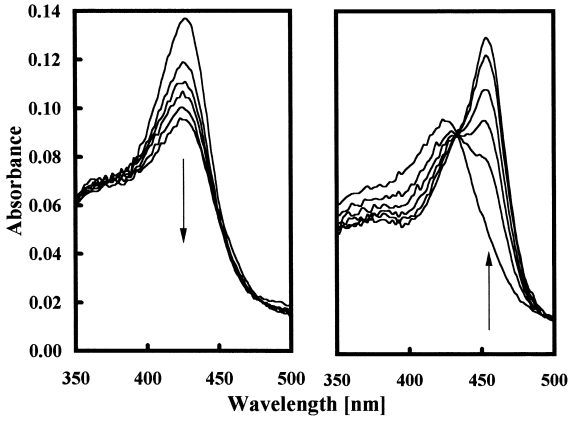

Fig. 1. Reaction of native MPO with PAA. Native MPO (2 μM heme) was mixed with 100 μM PAA. The first spectrum was taken 1.3 ms after mixing, subsequent spectra at 6.4, 8.9, 12, 16, 30 ms (left section) and 30, 152, 288, 510, 1020, 2000 ms (right section). The reaction was carried out in 100 mM phosphate buffer, pH 7, and 15°C.

3. Results and discussion

3.1. Compound I formation

When native ferric MPO was mixed with both aliphatic and aromatic peroxides, sequential formation of compound I and compound II was observed. MPO compound I is characterized by both peak broadening in the Soret region as well as a decrease in the extinction coefficient at 430 nm [8]. A good spectrum of compound I was formed within 30 ms when MPO (4 μM heme) was mixed with 200 μM PAA in the conventional stopped-flow mode (Fig. 1A, left section). Similar to previous observations with hydrogen peroxide as substrate [6–8], an excess of PAA was necessary for complete formation of compound I which was converted directly into compound II. Compound II exhibited a Soret maximum at 456 nm and an extinction coefficient at 456 nm of about 90% of that at 429 nm (Fig. 1A, right section). The isosbestic point between compound I and compound II was determined to be at 433 nm. Compound II formation was much slower than compound I formation. This was underlined by following the time course of the reaction at 429 nm, the Soret maximum of ferric MPO (not shown). Within the first 30 ms, there was a rapid decrease due to compound I formation, followed by a much slower phase of decrease as a result of compound II formation. The time course at 433 nm was monophasic, exhibiting only the first fast phase (not shown). Thus, this wavelength was used to study the dependence of the k_{obs} values from the peroxide concentration.

With the other aliphatic and aromatic hydroperoxides similar spectral changes were obtained and the time traces at 433 nm were also monophasic and exhibited a single-exponential behavior. With PAA, the forward second-order rate constant (k_f) at pH 7, obtained from the slope of the plot of k_{obs} versus concentration, was determined to be $(2.7 \pm 0.1) \times 10^6$ M^{-1} s^{-1} at 15°C (Fig. 2A). The intercept of this plot, (37 ± 3) s^{-1}, represents the reverse rate constant (k_b). The ratio of the rate constants, k_b/k_f, gave a value for the dissociation constant (K_d) of compound I to native enzyme and PAA of 15.1 μM. Table 1 summarizes the corresponding rate constants for the other peroxides. With the exception of *t*-butyl hydroperoxide ($(7.3 \pm 0.1) \times 10^3$ M^{-1} s^{-1}; $K_d = 7.5$ mM), all peroxides showed appreciable reactivity towards ferric MPO. The calculated rates for the reactions with H_2O_2 and ethyl hydroperoxide confirmed the data published in [6,8] within experimental error. Interestingly, peroxy acids were very effective in mediating this two-electron oxidation step of the protein. For comparison, 3-chloroperoxybenzoic acid (3-CPBA) ($(1.2 \pm 0.1) \times 10^7$ M^{-1} s^{-1}; $K_d = 6.9$ μM) was 10 times more effective than cumene hydroperoxide ($(1.2 \pm 0.1) \times 10^6$ M^{-1} s^{-1}; $K_d = 97$ μM) whereas compound I formation with PAA was about five times faster than with ethyl hydroperoxide ($(5.2 \pm 0.2) \times 10^5$ M^{-1} s^{-1}; $K_d = 161$ μM).

Fig. 2B shows the pH dependence of the apparent second-order rate constant for the reaction of native ferric MPO with PAA. The values of k_b were pH-independent within experimental error. The linear relationship between the logarithm of

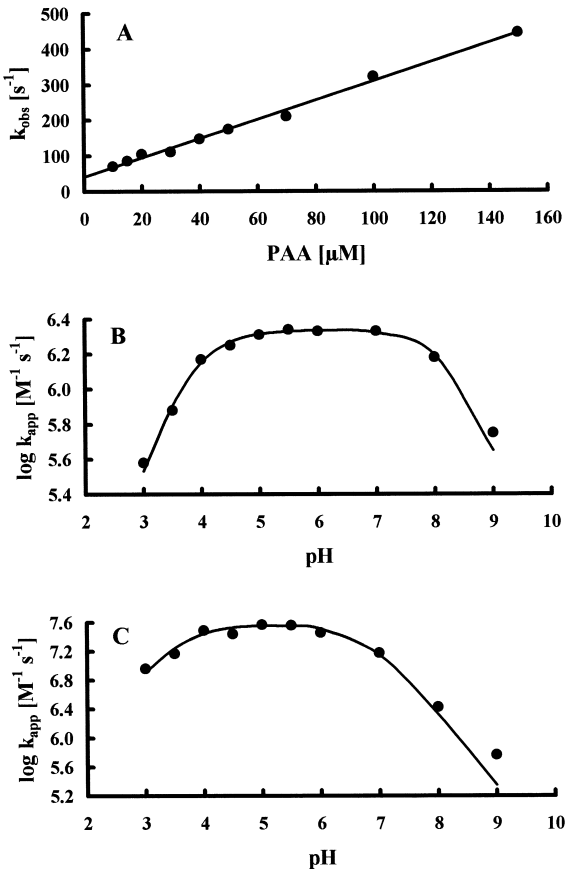

Fig. 2. A: Pseudo-first-order rate constants for compound I formation plotted against PAA concentration. Final enzyme concentration was 1 μM heme in 100 mM phosphate buffer, pH 7. Reaction was followed at 433 nm. The bimolecular rate constant was calculated from the slope. B: pH dependence of the apparent second-order rate constant of the reaction of MPO (0.5 μM heme) with PAA. Reactions were carried out in 100 mM phosphate–citrate buffer (pH 3–7), 100 mM phosphate buffer (pH 7–8) and 100 mM carbonate buffer (pH 8–9) at 15°C. The curve was computed on the basis of best-fit parameters from Eq. 1. C: pH dependence of the apparent second-order rate constant of the reaction of MPO (0.5 μM heme) with 3-CPBA. Conditions as in B. The curve was computed on the basis of best-fit parameters from Eq. 1.

k_{app} and pH at lower pH values indicated that an ionizable group on the enzyme could contribute to this behavior. Only when this group was in its conjugated base form, MPO reacted with PAA. The linear relationship between the logarithm of k_{app} and pH at higher pH values indicated that only PAA in its protonated form reacts with the enzyme.

The data points in Fig. 2B were fitted to the following equation (Eq. 1) on the basis of best-fit parameters:

$$k_{app} = \frac{k_{int}}{\left(1 + \frac{[H^+]}{K_1}\right) \times \left(1 + \frac{K_2}{[H^+]}\right)} \quad (1)$$

where k_{int} is the pH-independent second-order rate constant, K_1 is the dissociation constant of an ionizable group of the enzyme and K_2 is the dissociation constant of the substrate.

Eq. 1 yielded a k_{int} value of $(2.2 \pm 0.1) \times 10^6$ M^{-1} s^{-1} and pK_1 and pK_2 values of (3.7 ± 0.6) and (8.4 ± 0.6), respectively. Since the pK_a of PAA is 8.2 [10], it is clear that pK_2 is due to the dissociation of PAA.

The pH profile of the reaction of ferric MPO with 3-CPBA was similar (Fig. 2C), yielding a k_{int} value of $(3.6 \pm 0.2) \times 10^7$ M^{-1} s^{-1} and pK_1 and pK_2 values of (3.5 ± 0.2) and (7.1 ± 0.7), respectively, indicating that the decrease in activity at basic pH could be due to deprotonation of 3-CPBA (pK_a is 7.8 [10]). These findings demonstrate that also with aliphatic and aromatic peroxy acids compound I formation is controlled by the protonation state of a distal ionizable group, most likely His 95 [11], as has been demonstrated for the reaction with hydrogen peroxide [6,8]. The peroxides have to be in the protonated form in order to promote reaction.

3.2. Compound II formation

As has been outlined above, upon addition of peroxides to ferric MPO, sequential formation of compound I and compound II was observed. Fig. 3A shows the decay of compound I formed by a 10-fold excess of H_2O_2 within the first 4 s. As the time traces in Fig. 3C demonstrate, both a red shift to 456 nm (compound II) as well as a re-increase at 430 nm were observed, indicating that, besides the well known one-electron oxidation of hydrogen peroxide by compound I [6,8], some compound I reacted back to the ferric enzyme giving evidence for the reversibility of Reaction 1. On the contrary, when excess H_2O_2 or other peroxides were added to compound I in the multi-mixing stopped-flow mode, compound II was formed completely. An example is shown in Fig. 3B,D for the reaction between compound I and peroxoacetic acid. The direct spectral transition from compound I to compound II with a defined isosbestic point at 433 nm is shown. Similar spectral changes were obtained with all investigated hydroperoxides. Since in all cases there was a linear dependence of the

Table 1
Apparent second-order rate constants[a] for reactions of native ferric MPO and compound I with aliphatic and aromatic hydroperoxides at pH 7 and 15°C

Hydroperoxide	Compound I formation k_{app} (M^{-1} s^{-1})	Compound II formation k_{app} (M^{-1} s^{-1})
Hydrogen peroxide[b]	$(1.4 \pm 0.1) \times 10^7$	$(4.4 \pm 0.2) \times 10^4$
PAA	$(2.7 \pm 0.1) \times 10^6$	$(3.1 \pm 0.4) \times 10^3$
Ethyl hydroperoxide[c]	$(5.2 \pm 0.2) \times 10^5$	$(1.0 \pm 0.01) \times 10^4$
t-Butyl hydroperoxide	$(7.3 \pm 0.1) \times 10^3$	$(1.3 \pm 0.01) \times 10^2$
3-CPBA	$(1.8 \pm 0.1) \times 10^7$	$(6.6 \pm 0.3) \times 10^4$
Cumene hydroperoxide	$(1.2 \pm 0.1) \times 10^6$	$(1.6 \pm 0.2) \times 10^4$

[a]Second-order rate constants were calculated from the slope of the plot of the mean k_{obs} values versus substrate concentration. For details see Section 2.2.
[b]Compound I formation by hydrogen peroxide was published to be 2.3×10^7 M^{-1} s^{-1} (10°C) [6] and 1.8×10^7 M^{-1} s^{-1} (25°C) [8] at pH 7. Compound II formation was published to be 3.5×10^4 M^{-1} s^{-1} [7] and 8.2×10^4 M^{-1} s^{-1} [8] at 25°C and pH 7.
[c]Compound I formation by ethyl hydroperoxide was published to be 2.8×10^5 M^{-1} s^{-1} at 10°C and pH 7 [6].

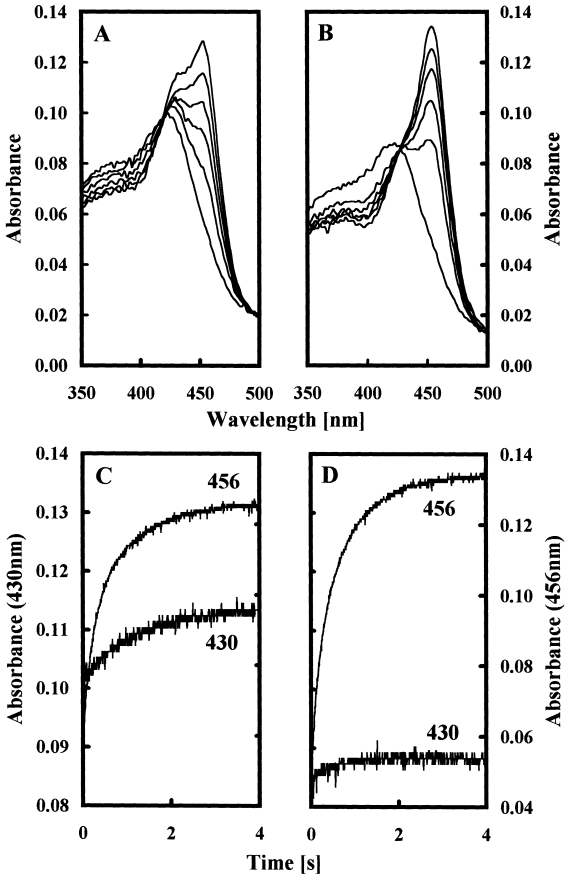

Fig. 3. A: Spectra of MPO compound I (2 μM heme) after adding buffer. Compound I was formed by mixing MPO (8 μM heme) with 80 μM hydrogen peroxide in the sequential-mixing mode and waiting for 20 ms. Reaction was carried out in 100 mM phosphate buffer, pH 7, at 15°C. The first spectrum was taken 4 ms after mixing compound I with buffer, subsequent scans at 100, 255, 485, 1002 and 4090 ms. B: Spectra of MPO compound I (2 μM heme) after adding 200 μM PAA. The first scan was taken 4 ms after adding PAA, subsequent scans at 255 ms, 516 ms, 905 ms, 11.4 s and 40 s. Conditions as in A. C: Time courses of the reaction which occurs when compound I is mixed with buffer at 430 and 456 nm. Conditions as in A. D: Time courses of the reaction between compound I and 200 μM PAA at 430 and 456 nm. Conditions as in B.

calculated k_{obs} values from the peroxide concentration (Fig. 4A), it is reasonable to assume that MPO compound I is able to oxidize both aliphatic and aromatic peroxides and peroxy acids in one-electron reactions yielding superoxide radicals in case of hydrogen peroxide or peroxyl radicals in case of the other organic hydroperoxides. The calculated rate constants are summarized in Table 1. With H_2O_2 as electron donor, a second-order rate constant of $(4.4 \pm 0.2) \times 10^4$ M^{-1} s^{-1} at pH 7 and 25°C was calculated which fits well to the recently published data [7,8]. With the exception of *t*-butyl hydroperoxide, the determined rates varied by a factor of about 20. Similar to oxidation of ferric MPO, hydrogen peroxide and 3-CPBA were most effective in compound I reduction.

As can be seen in Fig. 4B,C, there was again a distinct effect of pH on compound II formation. The curves plotted in Fig. 4B,C indicate that a single residue was involved in the reaction of compound I with both PAA and 3-CPBA, whereas at basic pH another proton-dependent process took place. Fitting these data to Eq. 1 on the basis of best-fit parameters yielded a k_{int} of $(3.7 \pm 0.2) \times 10^3$ M^{-1} s^{-1} (PAA) and $(2.7 \pm 0.2) \times 10^5$ M^{-1} s^{-1} (3-CPBA). The calculated pK_1 values were (4.8 ± 0.5) (PAA) and (4.0 ± 0.4) (3-CPBA), whereas the pK_2 values were calculated to be (9.2 ± 0.5) (PAA) and (6.8 ± 0.5) (3-CPBA), respectively. Thus, on the basis of the same reasoning as for compound I formation, the mechanism for the reduction of compound I by organic peroxides in their protonated form involves a distal ionizable group (most probably again His 95).

3.3. Conclusion

MPO has been shown to catalyze the decomposition of organic hydroperoxides. Two enzyme intermediates are involved. In the first case, the hydroperoxide undergoes a two-electron reduction to its corresponding alcohol and heme iron is oxidized to compound I. This species could then abstract hydrogen, producing a peroxyl radical and compound II. Both reactions are most effective around pH 7.

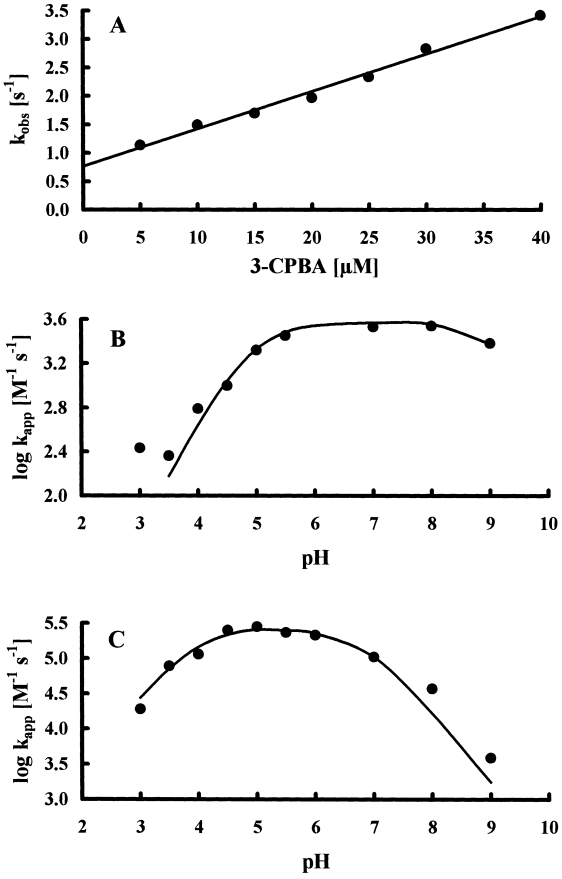

Fig. 4. A: Pseudo-first-order rate constants for compound II formation plotted against 3-CPBA concentration. Final enzyme concentration was 1 μM heme in 100 mM phosphate buffer, pH 7. Reaction was performed in the sequential-mixing mode as described in Section 2.2. The pH-dependent bimolecular rate constant was calculated from the slope. B: pH dependence of the apparent second-order rate constant of the reaction of MPO compound I (0.5 μM heme) with PAA. Reactions were carried out in 100 mM phosphate–citrate buffer (pH 3–7), 100 mM phosphate buffer (pH 7–8) and 100 mM carbonate buffer (pH 8–9) at 15°C. The curve was computed on the basis of best-fit parameters from Eq. 1. C: pH dependence of the apparent second-order rate constant of the reaction of MPO compound I (0.5 μM heme) with 3-CPBA. Conditions as in B. The curve was computed on the basis of best-fit parameters from Eq. 1.

Our findings demonstrate that the one-electron oxidation of hydroperoxides by MPO can be relevant in vivo as long as suitable co-substrates are present which reduce compound II and, thus, complete the peroxidase cycle. Then the high oxidation capacity of MPO compound I could be exploited to catalyze the formation of peroxyl radicals which could be responsible for the observed cytotoxicity of organic hydroperoxides.

References

[1] Klebanoff, S.J. (1991) in: Peroxidases in Chemistry and Biology (Everse, J., Everse, K.E. and Grisham, M.B., Eds.), pp. 1–35, CRC Press, Boca Raton, FL.
[2] Klebanoff, S.J. (1967) J. Clin. Invest. 46, 1078.
[3] Kimura, S. and Ikeda-Saito, M. (1988) Proteins Struct. Funct. Genet. 3, 113–120.
[4] Fenna, R., Zeng, J. and Davey, C. (1995) Arch. Biochem. Biophys. 316, 653–656.
[5] Furtmüller, P.G., Burner, U. and Obinger, C. (1998) Biochemistry 37, 17923–17930.
[6] Bolscher, G.J.M. and Wever, R. (1984) Biochim. Biophys. Acta 788, 1–10.
[7] Hoogland, H., Dekker, H.L., van Riel, C., Kuilenburg, A., Muijsers, A.O. and Wever, R. (1988) Biochim. Biophys. Acta 955, 337–345.
[8] Marquez, L.A., Huang, J.T. and Dunford, H.B. (1994) Biochemistry 33, 1447–1454.
[9] Chamulitrat, W., Cohen, M.S. and Mason, R.P. (1991) Free Radic. Biol. Med. 11, 439–445.
[10] Parker, W.E., Witnauer, L.P. and Swern, D. (1957) J. Am. Chem. Soc. 79, 1929–1931.
[11] Fiedler, T.J., Davey, C.A. and Fenna, R.E. (2000) J. Biol. Chem. 275, 11964–11971.